Magnetically Suspended Contact-Free Linear Actuator for Precision Stage

Sang Heon Lee*
Graduated student in Department of Mechanical Engineering, Yonsei University, Seoul 120-749, Korea
Yoon Su Baek
School of Mechanical Engineering, Yonsei University, Seoul 120-749, Korea

With the development of precision manufacturing technologies, the importance of precision positioning devices is increasing. Conventional actuators, dual stage or mechanically contacting type, have limitation in coping with performance demands. As a possible solution, magnetic suspension technology was studied. Such a contact-free system has advantages in terms of high accuracy, low production cost and easy adaptability to high precision manufacturing processes. This paper deals with magnetically suspended multi-degrees of freedom actuator which can realize large linear motion. In this paper, the operating principle is explained with the magnetic force analysis, and the equations of motion are derived. Experimental results of the implemented system are also given.

Key Words : Magnetic Suspension, Contact-free Linear Actuator, Precision Stage, Magnetic Circuit

1. Introduction

In tandem with the development of micro automation and circuit integration in semiconductor manufacturing processes and the higher demand for thin film transistor liquid crystal display (TFT-LCD) and plasma display panels (PDP), the importance of high precision position device is also increasing. Also, with the enlargement of the size of wafer for semiconductor and display panel, industries are demanding precision actuators that can generate high precision and large work range at the same time with simple structure.

There have been various kinds of research that have attempted to address such demands. As one formal result, the dual servo (fine/coarse) system has shown many possibilities, through its good performance in fine motion control by piezoelectrical actuator. But for a larger work range, this dual servo structure has shown a performance decrease, owing in part to its complex structure. Therefore, the main research current is towards the single servo system.

The aforementioned manufacturing processes are affected by the environment within which such processes occur. So the operations are generally executed in clean, sterile, vacuum rooms. To satisfy this environmental condition, the actuator must exclude all potential sources of contaminants and pollution. In view of such environmental needs, contact-free systems are preferable. This is because such systems (1) do not involve mechanical friction - thereby eliminating the necessity for lubrication - (2) are less likely to be affected by dust particles, and (3) have lower costs of production - through elimination of finishing work.

There are two methods to realizing a contact-

* Corresponding Author,
E-mail : shlee1@yonsei.ac.kr
TEL : +82-2-2123-4407; **FAX** : +82-2-362-2736
Graduated student in Department of Mechanical Engineering, Yonsei University, Seoul 120-749, Korea. (Manuscript **Received** October 31, 2002; **Revised** March 11, 2003)

free system. The first method is by using fluid and the other is by using electromagnetic force. Because the flows of fluid can be a form of disturbance as well as a source of pollution - from moisture and compressor oils - the second method is preferable, and can be expected to well satisfy industrial demands and needs.

The first contact-free actuator is the Sawyer motor, named after its inventor. This motor is levitated by multi air bearings and generates planar motion through electromagnetic forces. This system is still being adapted to bed for machining centers (Michael et al., 1999). Trumper and Won-Jong Kim have done research on the magnetically levitated planar actuator. They developed a precision stage that can generate 50×50 mm planar motion, $\pm 200\ \mu$m vertical translation, and $\pm 600\ \mu$ rad rotation about each axis using four linear motor (Kim et al., 1998). Jung, Lee and Baek have developed various contact-free surface actuators using levitation and suspension (Jung and Baek, 2001 ; Jung et al., 2002). Chung and Higuchi, on the other hand, have done research on contact-free linear actuators. Chung has developed variable reluctance (VR) type linear actuator for a magnetic levitated train (Liu and Sheu, 1996), and Higuchi has studied the suspension and propulsion of nonmagnetic material using electrostatic force (Jin and Higuchi, 1997). But, these studies have focussed on the development of moving systems instead of precision stage, so they have not dealt with positioning performance.

In this paper, we propose a suspension type contact-free linear actuator, using electromagnetic force between direct current electromagnet and conductor. This paper is structured in the following way. In chapter two, we analyze the magnetic force using magnetic circuit theory, and explain the operating principle and design of structure in chapter three. In chapter four, we derive an equation of motion, and we treat the control system with this result in chapter five. And finally, we verify the feasibility of the proposed system with experimental results and derive a conclusion.

2. Force Analysis

There are two magnetic field effects resulting in the production of mechanical forces. The first is alignment of flux lines, and the other is interaction between magnetic fields and current-carrying conductors. The second effect is generally called Lorentz force. For the Lorentz force, the magnitude of force is proportional to magnitude of magnetic field density and current flowing through the coil. The magnetic field is generated using rare earth (NdBFe) magnet stronger than ferrite magnet by 3 times. But when large magnetic forces are required, the high current causing thermal problem is required. The first method - generally called the variable reluctance (VR) principle - uses high permeability material. Therefore it is easy to generate strong magnetic force with low current and it is free from thermal problem. But it is difficult to say which principle is more preferable, because Lorentz force can produce attractive and repulsive different from VR principle. Therefore, it is necessary to choose best solution for final object.

In this study, we plan to develop precision positioning device for work in the ultra clean and vacuum environment so we select the VR principle free from thermal problem. The magnetic force by VR principle can be analyzed by magnetic circuit theory. The magnetic circuit theory is to translate continuous magnetic field phenomenon to equivalent distributed parameter system and applied to design electromagnetic systems. We adopt magnetic circuit theory to analyze magnetic force by basic magnetic element composing the proposed system.

2.1 Magnetic circuit theory

Using magnetic circuit theory, the one pair of electromagnet and ferromagnetic can be translated to equivalent magnetic circuit like Fig. 1. We can drive the governing equation like Kirchhoff's circuit law of electric circuit in the magnetic circuit using Ampere's circuital law (Roters, 1951). As we expected, the magnetic circuit is analogous to the electric circuit, but there are some differ-

ences. In the magnetic circuit, there exist magnetic effects of fringing and leakage flux, so analysis method is a little different. But because the fringing and leakage flux can be modeled, these effects do not much affect the analysis procedure. We ignore leakage flux for simplicity but in fact the leakage flux is too small to be significant, so only the fringing effect is considered.

The flux in the air gap is composed of multi flux tubes like Fig. 1(b), and each reluctance of flux tube is defined like below

$$R_1=\frac{z}{\mu_0(w_t-x)h} \tag{1}$$

$$R_2=\frac{1}{0.54\mu_0 h} \tag{2}$$

$$R_3=\frac{\pi}{2\mu_0 h\log_e\left(1+\frac{2x}{z}\right)} \tag{3}$$

where μ_0 is a permeability of air, w_t is width of pole, and h is length of pole.

If we connect each reluctance in parallel, the total reluctance in the air gap can be expressed like Eq. (4) using Eqs. (1)-(3).

$$R_g(x, z)=\left(\frac{1}{R_1}+\frac{2}{R_2}+\frac{2}{R_3}\right)^{-1} \tag{4}$$

If we assume that the relative permeability of ferromagnetic, the reluctance of ferromagnetic can be ignored. Therefore the Ampere's circuital law can be expressed as followings (Griffiths, 1989);

$$\oint \mathbf{H}\cdot d\mathbf{l}=\phi R_g=Ni \tag{5}$$

where ϕ is magnetic flux, N is coil turns, and i is current flowing through the path.

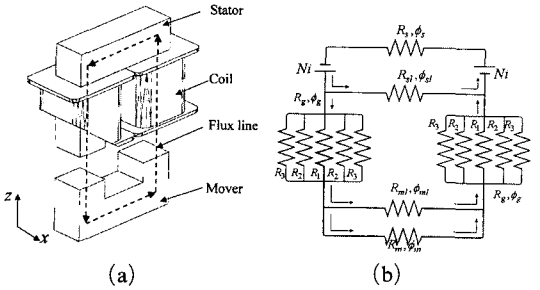

Fig. 1 Magnetic element (a) electromagnet and iron core (b) equivalent magnetic circuit

And the stored magnetic energy in the air gap can be derived like following

$$W_m=\frac{1}{2}L_i^2=\frac{1}{2}\frac{N^2i^2}{R_g} \tag{6}$$

where $L=N\phi/i$ means an inductance of closed circuit.

2.2 Magnetic force

By the energy conservation law, the variation of the stored magnetic energy causes the mechanical work (Nasar, and Unnewehr, 1983). With this fact, we can get the horizontal and vertical force using principle of virtual work like below

$$f_x(x, z, i)=-\frac{\partial W_m}{\partial x}=-\mu_0 N^2 i^2 h\left(\frac{4}{\pi x+2z}\right) \tag{7}$$

$$f_z(x, z, i)=-\frac{\partial W_m}{\partial z}=-\mu_0 N^2 i^2 h\left(\frac{x-l}{z^2}+\frac{8(1-(\pi x+2z)/2z)}{\pi(\pi x+2z)}\right) \tag{8}$$

We executed verification experiment before adopting derived theoretical equation. Fig. 2 shows the experimental setup. With constant current, the force was measured while changing relative position between electromagnet and ferromagnetic using micro stage and 6 d.o.f. force/torque sensor was used to measure magnetic force.

Fig. 3 shows the experimental results of normal force for suspension. The theoretical and experimental results are well agreed in our interesting

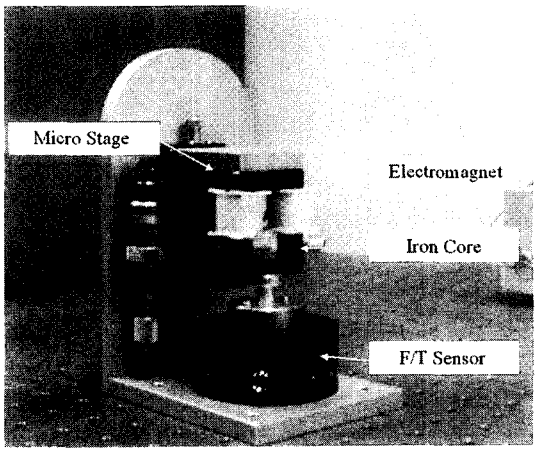

Fig. 2 Experimental setup for force calibration

point. But as the air gap decreases, the error increases in Fig. 3(a). As seen in the Eq. (8), the magnetic force is inversely proportional to the square of air gap, so when the air gap is too large, the high current is required and this high current causes the thermal problem and magnetic saturation of magnetic material. From Fig. 3(a), we can decide the appropriate nominal position to get a more exact theoretical equation and proper current to suspension by avoiding part depicted circle in the Fig. 3(a). We set the nominal air gap length as 1700 μm. Fig. 3(b) shows the horizontal force. As the x displacement increases, the gradient of force gets constant. This means that we can get the constant horizontal force by appropriate pole arrangement.

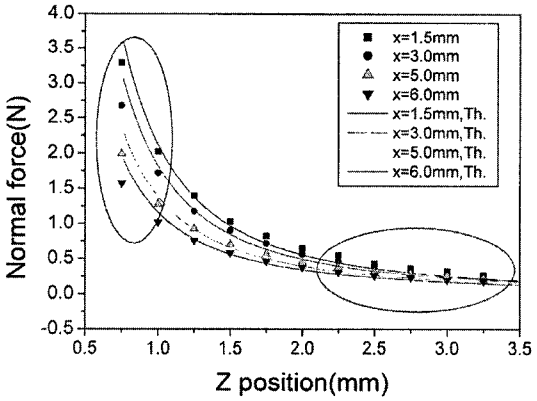

(a)

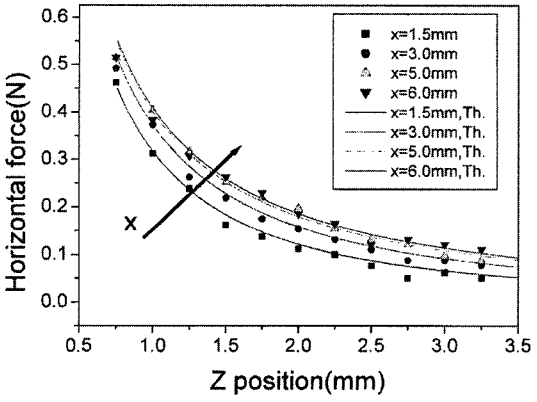

(b)

Fig. 3 Experimented results (a) normal force (b) horizontal force

3. Structure and Operating Principle

3.1 Structure

There are two kinds of possible structure to set up the proposed system. The first is moving electromagnet type and the other is moving ferromagnetic type. For the first structure, it is impossible to perfect suspension and isolation from the environment because of wiring to power source. Therefore the moving ferromagnetic type was chosen and the mover is entirely isolated. Fig. 4 shows the structure of proposed system. The stator is composed of 12 electromagnets and the mover is composed of 8 passive poles. Totally, 5 non-contact displacement sensors are used. Three capacitance type gaps sensors under the mover measure out of plane motion and two laser sensor measure in plane motion.

3.2 Operating principle

The operating principle of the proposed system is similar to that of VR type linear motor but it is different in the view of the function of normal force. The conventional VR type linear motor is constrained by LM guide, so the excessive normal force damages the guide and should be avoided. But the normal force in the proposed system is the main force for stable suspension and is related to propulsive force, so the normal force should be distributed properly.

Fig. 5 shows the operating principle. In Fig. 5

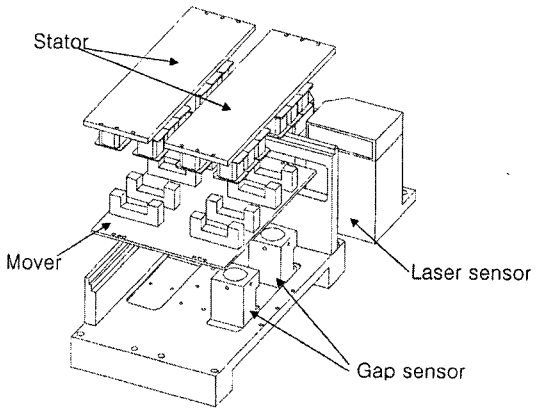

Fig. 4 Schematic diagram of developed system

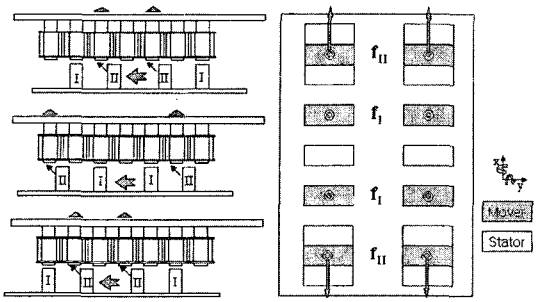

Fig. 5 Operating principle (a) translation (b) positioning

(a), the electromagnets of stator are excited by nominal current to suspend mover stably in static position and when the currents for electromagnets located near the mover pole II (depicted triangle) increase, the mover starts to translate to left direction and when the currents for electromagnets located near the mover pole I (depicted triangle) increase, the mover keep translating to left direction. With this sequence of exciting current, the mover makes translation. Fig. 5(b) shows the distribution of magnetic force from top. With the combination of normal and horizontal forces, the 3 dof out of plane motion and 2 dof in plane motion are possible in the proposed system. The translation in transversal direction is passively controlled by the guidance force, which is characteristic of VR type actuator, but if the disturbance to this direction is stronger than the guidance force, the additional actuator is required for active control. In this study, we do not take much account of transversal disturbance, but when we expand this linear actuator to planar actuator, it is possible to control 6 dof motion by combination of the proposed linear actuator.

4. System Modeling

The proposed system is nonlinear but it can be linearized as a function of displacement and current in a small range around a point.

4.1 Linearization of magnetic forces

In order to derive equation of motion and to adapt linear control theories, the force should be linearized. The magnetic force is the function of displacement and current as shown Eqs. (7) and (8). And the magnetic force can be classified into three kinds with respect to relative position between the stator and mover pole. The first case is that the stator pole leads the mover pole, the second is that the mover pole leads the stator pole, and the last is that the stator and the mover poles are aligned. Therefore the magnetic force can be expressed the followings.

$$\mathbf{f}^a=\mathbf{f}_{j1}(x,\ z,\ i)=\mathbf{f}_{j5}(x,\ z,\ i) \tag{9.a}$$

$$\mathbf{f}^b=\mathbf{f}_{j2}(x,\ z,\ i)=\mathbf{f}_{j6}(x,\ z,\ i) \tag{9.b}$$

$$\mathbf{f}^c=\mathbf{f}_{j3}(x,\ z,\ i)=\mathbf{f}_{j4}(x,\ z,\ i) \tag{9.c}$$

where, j is subscript of row for 1 and 2, and a, b, and c mean the state of stator leading , mover leading, and aligned respectively.

Linearizing Eq. (9) at a nominal position and neglecting the second order or higher order terms under the small range assumption and simplifying, we can get the following equations.

$$f_{j1x}=f_{j5x}=K^a_{xx}x+K^a_{xz}z+K^a_{xi}i \tag{10.a}$$

$$f_{j2x}=f_{j6x}=K^b_{xx}x+K^b_{xz}z+K^b_{xi}i \tag{10.b}$$

$$f_{j3x}=f_{j4x}=K^c_{xx}x+K^c_{xz}z+K^c_{xi}i \tag{10.c}$$

$$f_{j1z}=f_{j5z}=K^a_{zx}x+K^a_{zz}z+K^a_{zi}i \tag{10.d}$$

$$f_{j2z}=f_{j6z}=K^b_{zx}x+K^b_{zz}z+K^b_{zi}i \tag{10.e}$$

$$f_{j3z}=f_{j4z}=K^c_{zx}x+K^c_{zz}z+K^a_{zi}i \tag{10.f}$$

where

$$K_{xx}=\frac{\Delta f_x}{\Delta x}\bigg|_{x_0,z_0,i_0}\quad K_{xz}=\frac{\Delta f_x}{\Delta z}\bigg|_{x_0,z_0,i_0}\quad K_{xi}=\frac{\Delta f_x}{\Delta i}\bigg|_{x_0,z_0,i_0}$$

$$K_{zx}=\frac{\Delta f_z}{\Delta x}\bigg|_{x_0,z_0,i_0}\quad K_{zz}=\frac{\Delta f_z}{\Delta z}\bigg|_{x_0,z_0,i_0}\quad K_{zi}=\frac{\Delta f_z}{\Delta i}\bigg|_{x_0,z_0,i_0}$$

and the subscript 0 means the nominal value for position and current.

4.2 Equations of motion

In order to obtain equations of motion of the mover, we set the moving coordinate (x, y, z) on the mover and the reference coordinate (X, Y, Z) on the stator. Using the Z-Y-X Euler's angle, we can get the translational displacement and the rotational displacement. The homogeneous transformation matrix T can be expressed as follows,

with assumption of small displacement (Craig, 1989).

$$T=\begin{bmatrix} 1 & -\gamma & \beta & x \\ \gamma & 1 & -\alpha & y \\ -\beta & \alpha & 1 & z \\ 0 & 0 & 0 & 1 \end{bmatrix} \tag{11}$$

Setting the moving coordinate to the mass center of the mover and using Eq. (11) and the principle of linear momentum, we get the flowing equations of linear motion. We also get the equations of rotational motion using the same method and simplify equations ignoring the multiplied terms of small variables.

$$\Sigma f_z = m\ddot{z} \tag{12.a}$$
$$\Sigma f_x = m\ddot{x} \tag{12.b}$$
$$\Sigma M_x = I_x\ddot{\alpha} \tag{12.c}$$
$$\Sigma M_y = I_y\ddot{\beta} \tag{12.d}$$
$$\Sigma M_z = I_z\ddot{\gamma} \tag{12.e}$$

Therefore the equations of motion can be expressed as the following vector form.

$$\mathbf{F}=\mathbf{M}\ddot{\mathbf{q}} \tag{13}$$

where, $\mathbf{F}=[\Sigma f_z\ \Sigma f_x\ \Sigma M_x\ \Sigma M_y\ \Sigma M_z]^T$, $\mathbf{M}=\mathrm{diag}[m\ m\ I_x\ I_y\ I_z]$, $\mathbf{q}=[z\ x\ \alpha\ \beta\ \gamma]^T$

The sum of force and moment can be calculated using the definition in Fig. 6 as followings.

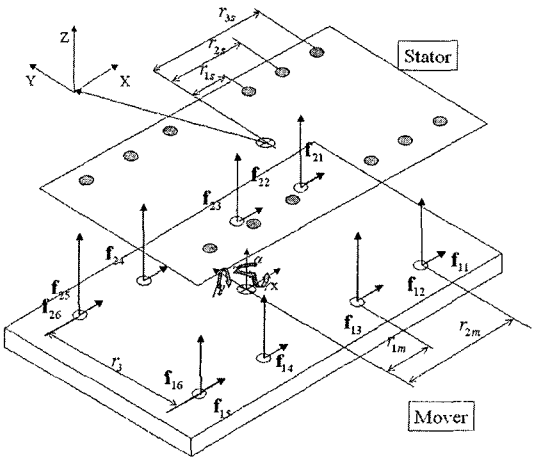

Fig. 6 Free body diagram of mover

$$\Sigma f_z = \sum_{i=1}^{2}\sum_{j=1}^{6} f_{ijz} \tag{14.a}$$

$$\Sigma f_x = \sum_{i=1}^{2}\sum_{j=1}^{6} f_{ijx} \tag{14.b}$$

$$\Sigma M_x = \frac{r_3}{2}\left(\sum_{j=1}^{6} f_{1jz} - \sum_{j=1}^{6} f_{2jz}\right) \tag{14.c}$$

$$\begin{aligned}\Sigma M_y = {} & r_{1m}(f_{13z}+f_{23z}-f_{14z}-f_{24z}) \\ & + r_{2m}(f_{11z}+f_{12z}+f_{21z}+f_{22z}-f_{15z} \\ & -f_{16z}-f_{25z}-f_{26z})\end{aligned} \tag{14.d}$$

$$\Sigma M_z = \frac{r_3}{2}\left(\sum_{j=1}^{6} f_{2jx} - \sum_{j=1}^{6} f_{1jx}\right) \tag{14.e}$$

In order to calculate forces acting on the mover, we obtain the relative displacement between stator and mover pole using homogeneous transformation from moving coordinate to reference coordinate as shown below.

$$\begin{aligned}\delta\mathbf{p}_{i1} &= [\delta p_{i1x}\ \ \delta p_{i1z}]^T \\ &= [r_{3s}-(-1)^{i+1}\gamma r_3+x-r_{2m}\ \ z-\beta r_{3s}+(-1)^{i+1}\alpha r_3]^T\end{aligned} \tag{15.a}$$

$$\begin{aligned}\delta\mathbf{p}_{i2} &= [\delta p_{i2x}\ \ \delta p_{i2z}]^T \\ &= [r_{2s}-(-1)^{i+1}\gamma r_3+x-r_{2m}\ \ z-\beta r_{2s}+(-1)^{i+1}\alpha r_3]^T\end{aligned} \tag{15.b}$$

$$\begin{aligned}\delta\mathbf{p}_{i3} &= [\delta p_{i3x}\ \ \delta p_{i3z}]^T \\ &= [r_{1s}-(-1)^{i+1}\gamma r_3+x-r_{1m}\ \ z-\beta r_{1s}+(-1)^{i+1}\alpha r_3]^T\end{aligned} \tag{15.c}$$

$$\begin{aligned}\delta\mathbf{p}_{i4} &= [\delta p_{i4x}\ \ \delta p_{i4z}]^T \\ &= [-r_{1s}-(-1)^{i+1}\gamma r_3+x+r_{1m}\ \ z+\beta r_{1s}+(-1)^{i+1}\alpha r_3]^T\end{aligned} \tag{15.d}$$

$$\begin{aligned}\delta\mathbf{p}_{i5} &= [\delta p_{i5x}\ \ \delta p_{i5z}]^T \\ &= [-r_{2s}-(-1)^{i+1}\gamma r_3+x+r_{2m}\ \ z+\beta r_{2s}+(-1)^{i+1}\alpha r_3]^T\end{aligned} \tag{15.e}$$

$$\begin{aligned}\delta\mathbf{p}_{i6} &= [\delta p_{i6x}\ \ \delta p_{i6z}]^T \\ &= [-r_{3s}-(-1)^{i+1}\gamma r_3+x+r_{2m}\ \ z+\beta r_{3s}+(-1)^{i+1}\alpha r_3]^T\end{aligned} \tag{15.f}$$

where $\delta\mathbf{p}_{i1}$ is the relative displacement between stator and mover pole 1 and i is subscript of raw for 1 and 2.

By substituting Eq. (15) to Eq. (10), the transformed force equation is like following

$$f_{ijx} = K^o_{xx}\,\delta p_{ijx} + K^o_{xz}\,\delta p_{ijz} + K^o_{xi}\,i_{ij} \tag{16.a}$$
$$f_{ijz} = K^o_{zx}\,\delta p_{ijx} + K^o_{zz}\,\delta p_{ijz} + K^o_{zi}\,i_{ij} \tag{16.b}$$

where i_{ij} is an input current for i and jth electromagnet and the superscript o is defined like these ; j=1, 5 o=a, j=2, 6 o=b , j=3, 4 o=c.

And finally we can derive the linearized equation of motion by substituting Eq. (16) to Eq. (14) and Eq. (13).

$$\mathbf{M}\ddot{\mathbf{q}}+\mathbf{K}\mathbf{q}=\mathbf{F}_c \tag{17.a}$$

where $\mathbf{K}$ and $\mathbf{F}_c$ are defined as Eq. (17.b) and

(17.c)

$$\mathbf{K}=\begin{bmatrix} 4K^{zz} & 4K^{zx} & 0 & 0 & 0 \\ 4K^{xz} & 4K^{xx} & 0 & 0 & 0 \\ 0 & 0 & 4r_3K^{zz} & 0 & -4r_{3s}K^{zx} \\ 0 & 0 & 0 & 4(-r_{1m}r_{1s}K^c_{zz}+r_{2m}r_{3s}K^a_{zz}+r_{2m}r_{2s}K^b_{zz}) & 0 \\ 0 & 0 & -4r_3(K^a_{xz}+K^b_{xz}) & 0 & 4r_{3s}K^{xx} \end{bmatrix} \quad (17.b)$$

where, $K^{zz}=(K^a_{zz}+K^b_{zz}+K^c_{zz})$, $K^{zx}=(K^a_{zx}+K^b_{zx}+K^c_{zx})$, $K^{xz}=(K^a_{xz}+K^b_{xz}+K^c_{xz})$, $K^{xx}=(K^a_{xx}+K^b_{xx}+K^c_{xx})$

$$\mathbf{F}_c=\begin{bmatrix} K^a_{zi}\left(\sum_{j=1}^{2} i_{j1}+i_{j5}\right)+K^b_{zi}\left(\sum_{j=1}^{2} i_{j2}+i_{j6}\right)+K^c_{zi}\left(\sum_{j=1}^{2} i_{j3}+i_{j4}\right) \\ K^a_{xi}\left(\sum_{j=1}^{2} i_{j1}+i_{j5}\right)+K^b_{xi}\left(\sum_{j=1}^{2} i_{j2}+i_{j6}\right)+K^c_{xi}\left(\sum_{j=1}^{2} i_{j3}+i_{j4}\right) \\ r_3\left(K^a_{zi}\left(\sum_{j=1}^{2}(-1)^{j+1}(i_{j1}+i_{j5})\right)+K^b_{zi}\left(\sum_{j=1}^{2}(-1)^{j+1}(i_{j2}+i_{j6})\right)+K^c_{zi}\left(\sum_{j=1}^{2}(-1)^{j+1}(i_{j3}+i_{j4})\right)\right) \\ r_{2m}K^a_{zi}\left(\sum_{j=1}^{2}(-1)^{j}(i_{j1}+i_{j5})\right)+r_{2m}K^b_{zi}\left(\sum_{j=1}^{2}(-1)^{j}(i_{j2}+i_{j6})\right)+r_{1m}K^c_{zi}\left(\sum_{j=1}^{2}(-1)^{j}(i_{j3}+i_{j4})\right) \\ r_3\left(K^a_{xi}\left(\sum_{j=1}^{2}(-1)^{j}(i_{j1}+i_{j5})\right)+K^b_{xi}\left(\sum_{j=1}^{2}(-1)^{j}(i_{j2}+i_{j6})\right)+K^c_{xi}\left(\sum_{j=1}^{2}(-1)^{j}(i_{j3}+i_{j4})\right)\right) \end{bmatrix} \quad (17.c)$$

From the derived equations of motion Eq. (17), we can find the fact that the proposed system has couplings between some degrees of motion like the characteristic of VR type actuator. In order to obtain stable suspension and precious motion, the degrees of coupling of motions should be reduced. It is possible to reduce degrees of coupling by decreasing the value of K^{xz} and K^{zx} in Eq. (17.b) in the process of design of pole shape and adopting optimal control theory. Because the study of reducing coupling is related with performance improvement, we put this study as a future work. We design the controller using the derived equations but this system is redundant that uses 12 electromagnets. Therefore the forces should be allocated in order to solve the equation of motion and calculate required control inputs. The details will be treated in the next chapter.

5. Hardware Implementation and Experimental results

5.1 Hardware implementation

As mentioned before, we used five noncontact displacement sensors. As the out of plane motion is small, we used capacitance type sensors (S600-2, Micro-Epsilon, 0.4 μm), and used laser sensors (ILD1400-100, Micro-Epsilon, 100 μm) for measuring large in plane motion. The laser sensor uses the principle of optical triangulation, so it can measure wide range but the resolution is lower than the capacitance type sensor. We can find this performance gap in the experimental results. The results of in plane motion have low quality. We control the system in concept of one stage using celeron pc. The command signal for feedback control and transformation sensor signal are generated by D/A(PCL-726, 12bit, Advantech), A/D(PCL-817, 100 KHz 16-bit, Advantech co.) board respectively. And we used 8 channels DC power amplifier (GA455p, Glentek) to

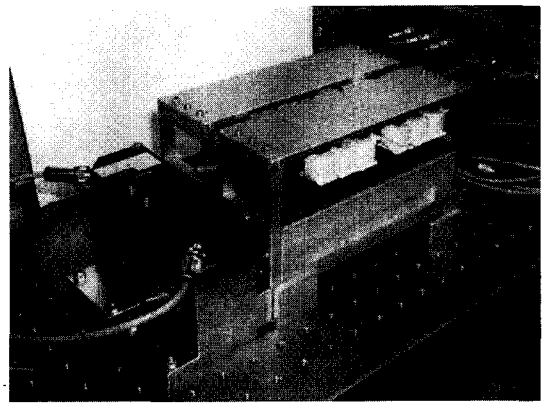

Fig. 7 Photograph of developed system

Table 1 Specification of developed system

Item		Symbol	Value
Fixed Stator	Pole width	w_t	10(mm)
	Pole thickness	l_t	10(mm)
	Pole pitch	τ	10(mm)
	Winding	Nx	335(turns)
Mover	Pole width	w_t	10(mm)
	Pole thickness	l_t	10(mm)
	Pole pitch 1	r_1	20(mm)
	Pole pitch 2	r_2	50(mm)
	Pole pitch 3	r_3	70(mm)
	Pole height	h_p	20(mm)
	Mass of mover	m	0.52(Kg)
	Moment of Inertia	I_x	7.58E-4(Kgm^2)
		I_y	7.68E-4(Kgm^2)
		I_z	1.51E-3(Kgm^2)

activate electromagnets. Fig. 7 shows the developed system. Table. 1 shows the main specification of the system. The translational operating range can be expanded by adding more electromagnets, but the developed system can moves 10 mm. In the stage of design, we did not optimal design technique, this specification shows much room for improvement.

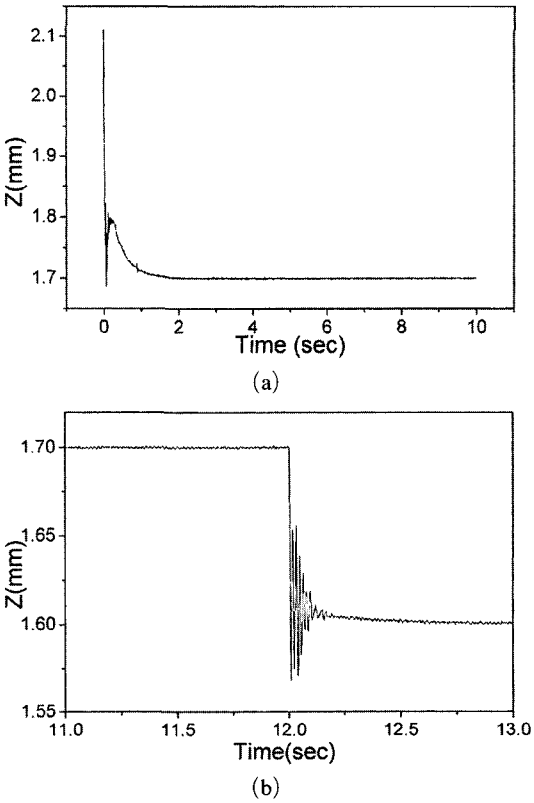

Fig. 8 Experimental results (a) suspension test (b) step response (100 μm)

5.2 Experimetal results

As mentioned before, this system is a redundant one so the force allocation is required and the suspension and propulsion forces change with displacement of mover, so it is difficult to keep suspension stable with constant force allocating ratio during translation. As given in the force calibration test, normal force is dominant in the stability of this system. Therefore, we focused on the force allocation of the out of plane mode D.O.F forces and allocated the magnetic force to act on the mover pole with rate of 2 : 3 : 3 : 2 for one row. The current exciting sequence for translation is similar to that of linear switched reluctance motor. The conventional PID controller is used with described force allocation during experiment.

The experiment was executed focusing on the feasibility of the proposed system for precision positioning. At first, we checked stability and positioning performance in the static position through x axis. Fig. 8(a) shows the result of the suspension experiment. The mover goes up from the initial position to nominal position stably. Fig. 8(b) is the response of 100 μm step input. The overshoot is about 20% and settling time is about 190 ms.

And we executed a horizontal direction translation test. Fig. 9 shows the response of trapezoidal command. Fig. 9(a) is for horizontal response and Fig. 9(b) is for vertical response. In Fig. 9(a), the periodic peaks are generated. This phenomenon is a result of the discontinuity of normal and horizontal force at the end of poles. It is considered that the fluctuation of force by edge effect causes this discontinuity. At the design stage, we largely did not take account of edge effects, so it was difficult to remove this periodic peak entirely. With these results, it looks hard to apply this system to scan-and-step type positioning system. But, with the next test results, we

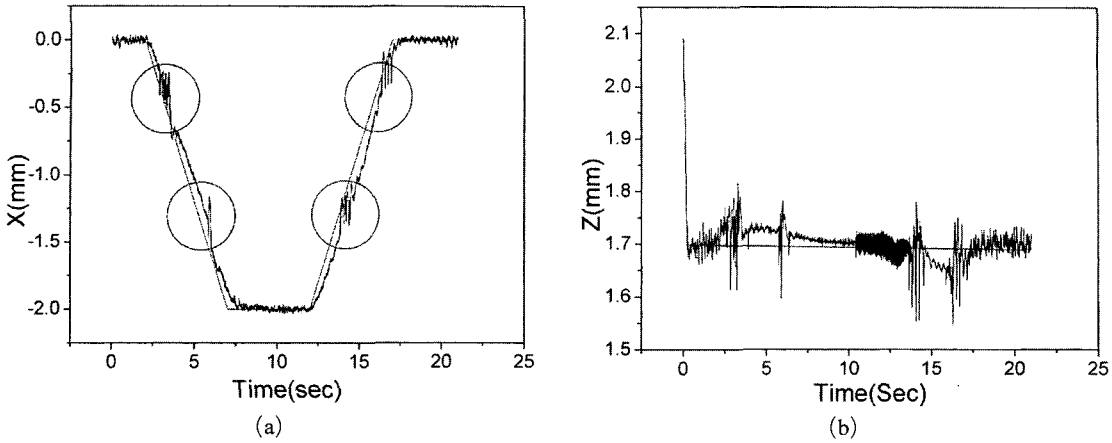

(a) (b)

Fig. 9 Trapezoidal linear motion test results (a) horizontal result (b) vertical result

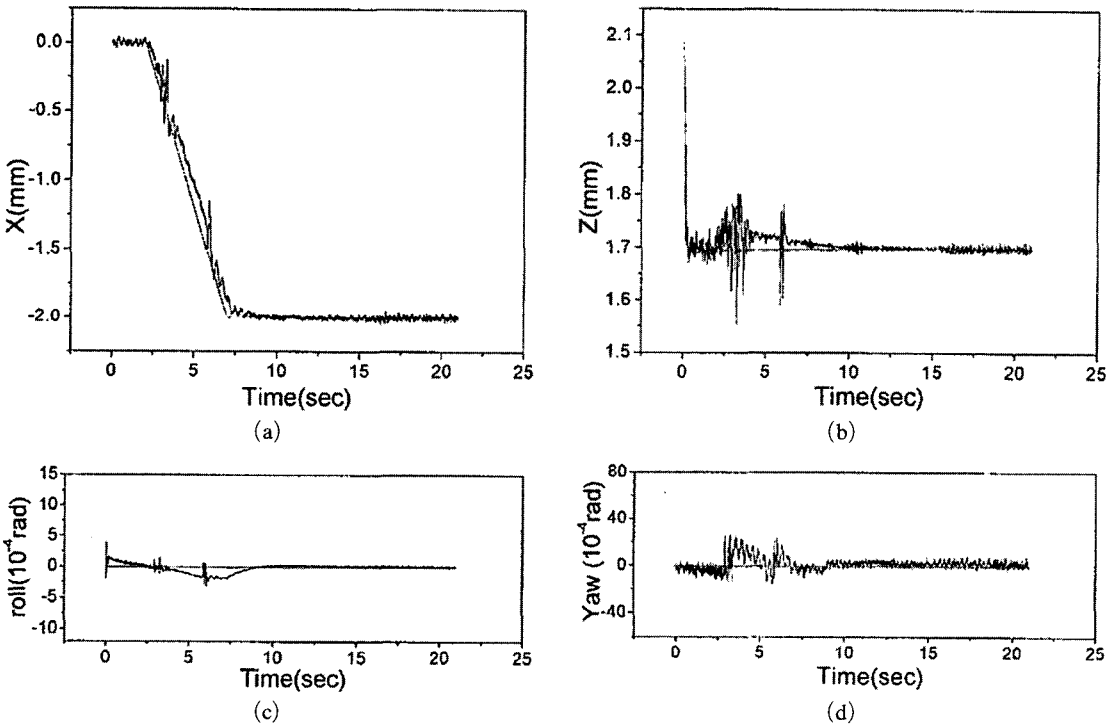

(a) (b) (c) (d)

Fig. 10 Experimental results of mation and keeping position (a) horizontal (b) vertical (c) roll (d) yaw

could assure some possibilities.

Fig. 10 shows the results of moving and keeping position test. In Fig. 10, while the mover translates, the result of each dof is coupled and shows low performance. But when the mover arrived at the target position, the system gets to stable. The steady state errors of each dof are ± 2 μm for horizontal translation, ± 5 μm for vertical translation, ± 10 μrad for pitch, ± 10 μrad for roll, and ± 300 μrad for yaw. The performance is not much satisfying but we could find the feasibility of applying this system to step-and-repeat type precision actuator from these results.

6. Conclusion

In this study, we proposed and developed the

magnetically suspended contact-free linear actuator for development of precision positioning device. As an advantage of the proposed system, the simple structure by the generation of simultaneous normal and horizontal force and the high possibility to expand dof to planar motion and operating range by adding electromagnets are proved. We executed some experiments to verify the feasibility of applying the proposed system to precision positiong devices. In view of the performance, the results were not wholly satisfying, but this system showed the possibility of application to step-and-repeat type system and much future work for performance enhancement, for example the identification of coupling between normal and horizontal force, and decoupling method. As solution of decoupling normal and horizontal force, we propose optimal design of pole shape and pitch and various control strategy e. g. control using transformation matrix like dq and fb transformation and optimal control. After the successful work, the proposed system would well satisfy industrial demands.

Acknowledgment

This work was supported by grant No. (R01-2000-00-00304-0, 2002) from Basic Research Program of Korea Science & Engineering Foundation (KOSEF).

References

Craig, J. J., 1989, *Introduction to robotics mechanic and control*, Addison-Wesley Publishing Company.

Griffiths, D. J., 1989, *Introduction to electrodynamics*, PRENTICE HALL.

Jin, J. and Higuchi, T., 1997, "Direct Electrostatic Levitation and Propulsion," *IEEE Trans. on Industrial Electronics*, Vol. 44, No. 2, pp. 234~239.

Jung, K. S. and Baek, Y. S., 2001, "Precision Stage Using A Novel Contact-Free Planar Actuator Based on Combination of Electromagnetic forces," *Trans. on KSME A*, Vol. 25, No. 11, pp. 1863~1872.

Jung, K. S., Lee, S. H. and Baek, Y. S., 2002, "Feasibility Study of General-purpose Precision Stage Using A Novel Contact-Free Surface Actuator Based on Magnetic Suspension Technology," *Trans. on KSME A*, Vol. 26, No. 3, pp. 452~460.

Kim, W. J., David, L. T., and Jeffrey, H. L., 1998, "Modeling and Vector Control of Planar Magnetic Levitator," *IEEE Trans. on Industry Applications*, Vol. 34, No. 6, pp. 1254~1262.

Lie, C. T. and Sheu, N., 1996, "Optimal Pole Arrangement Design of a Linear Switched-Reluctance Machine for Magnetic Levitation and Propulsion System," *IEEE Trans. on Magnetics*, Vol. 32, No. 5, pp. 5067~5069.

Michael, A., Soltz, Y., Yao, L. and Jehuda, I. S., 1999, "Investigation of a 2-D Planar Motor Based Machine Tool Motion System," *International Journal of Machine Tools and Manufacture*, Vol. 39, Issue 7, pp. 1157~1169.

Nasar, S. A., and Unnewehr, L. E., 1983, *Electromechanics and Electric Machines*, John Wiley & Sons, Inc.

Roters, H. C., 1951, Electromagnetic devices, John Wiley & Sons, Inc.